Climate variability and the shape of daily precipitation: A case study of ENSO and the American West

Nicole Feldl *

Department of Atmospheric Sciences, University of Washington, Seattle, Washington

Gerard H. Roe

Department of Earth and Space Sciences, University of Washington, Seattle, Washington

* *Corresponding author address:* Nicole Feldl, Department of Atmospheric Sciences, University of Washington, Box 351640, Seattle, WA 98195-1640.
E-mail: feldl@u.washington.edu

ABSTRACT

Characterizing the relationship between large-scale atmospheric circulation patterns and the shape of the daily precipitation distribution is fundamental to understanding how dynamical changes are manifest in the hydrological cycle, and it is also relevant to issues such as natural hazard mitigation and reservoir management. We pursue this general question, using ENSO variability and the American West as a case study. When considering the full range of wintertime precipitation, we find that, consistent with conventional wisdom, mean precipitation intensity is enhanced during El Niño relative to La Niña in the southwest, and vice versa in the northwest. We further attribute this change in mean to a shift in the distribution of daily precipitation towards more intense daily rainfall rates. In addition, we observe fundamental changes in the shape of the precipitation distributions, independent of shifts in the mean. Surprisingly, for intense precipitation, La Nina winters actually demonstrate a significant increase in intensity (but not frequency) across the southwest. A main lesson from this analysis is that, in response to ENSO variability, changes in extreme events can be significantly different from changes in the mean. In some instances, even the sign of the change is reversed. This result suggests that patterns of large-scale variability have an effect on the precipitation distribution that is nuanced, and cannot be regarded as simply causing a shift in climatic zones. It also raises interesting questions concerning how best to establish confidence in climate predictions.

1. Introduction

Understanding interannual and future changes in the hydrological cycle is of great importance to society. This is true both for planning the management of water resources and also for the mitigation of natural hazards, such as floods, landslides, and avalanches. In the case of water resources, it may be seasonal mean precipitation that is most important, while in the case of hazards, it is typically the occurrence of heavy or extremely heavy precipitation that matters. Depending on the application, the complete statistical distribution of precipitation frequency and intensity is of interest. The shape of the precipitation distribution is also a function of climate state, changing throughout the annual cycle as wintertime drizzle transitions to springtime showers and then to summertime storms. How are such factors manifest in the observational record of interannual variability and in model projections of climate change?

Understanding the dynamic and thermodynamic controls on precipitation remains a challenge in climate science. General circulation models (GCM) struggle to successfully simulate the observed distribution of precipitation intensity (Sun et al. 2006; Wilcox and Donner 2007; Allan and Soden 2007) or the satellite-derived precipitation response to sea surface temperature (SST) variability (Wentz et al. 2007; Allan and Soden 2008). Convective parameterization in models certainly plays a role in the discrepancy between observed and simulated precipitation. For example, Wilcox and Donner (2007) show that the choice of model convective parameterization has a larger impact on the statistics of heavy precipitation than a 2K warming. Nor are the statistics of stratiform precipitation adequately resolved (e.g Zhou et al. 2007). In light of these challenges, it is clearly worthwhile to characterize

the observed precipitation distributions as carefully as possible, in order to evaluate the skill of models used to predict future changes.

Recent studies have made impressive strides in understanding expected changes in global mean and extreme precipitation in a warmer climate, largely based on considerations of moisture availability and the global energy budget. While atmospheric water vapor content increases by close to 7% per degree of global mean temperature increase (i.e. 7% K^{-1}) in accordance with Clausius-Clapeyron scaling and assuming constant relative humidity, coupled climate models predict an increase in global mean precipitation of approximately 2% K^{-1}, consistent with energy balance constraints (Allen and Ingram 2002). The intensity of extreme precipitation events is expected to be broadly constrained by moisture availability and hence increase faster than global mean precipitation (Trenberth et al. 2003). However several studies argue that increases in intense precipitation should not scale exactly with Clausius-Clapeyron due to the additional effects of latent heat release, changes in circulation strength, and the difference between local mean temperature and the temperature at which precipitation extremes occur, although observations remain debated (Pall et al. 2007; O'Gorman and Schneider 2009; Lorenz and DeWeaver 2007). For example, in a series of idealized GCM experiments O'Gorman and Schneider (2009) show that fractional changes in precipitation extremes are less than changes in water vapor content, except at highest latitudes where the local temperature effect dominates.

Progress has also been made in understanding the regional patterns of predicted precipitation changes. Strengthening of tropospheric moisture fluxes, as predicted in a warmer climate, is expected to lead to an enhancement of the geographic distribution of evaporation and precipitation (Held and Soden 2006; Lorenz and DeWeaver 2007). In other words, wet

regions are expected to become wetter, and dry regions drier. This pattern is simulated in the Intergovernmental Panel of Climate Change (IPCC) Fourth Assessment Report multi-model ensemble projections, which indicate a general increase in mean precipitation in the tropics and mid-latitudes and a decrease in the already arid subtropics. Furthermore, climate models suggest that a wetter climate for a given region is one in which heavy precipitation is more intense and more frequent (Sun et al. 2007; Kharin et al. 2007). This is consistent with the theoretical argument for a shift in the precipitation distribution towards extremes under global warming. Given the predicted response of global and regional mean precipitation to warming, and the suggestion that increases in precipitation are accomplished by intense precipitation events, there remains a need to consider the full range of expected changes in the statistical precipitation distribution.

Impacts pertaining to these projected precipitation changes are likely to be far-reaching and significant. As discussed above, percent increases in intense precipitation per degree warming are generally expected to be larger than percent increases in the mean. Moreover all evidence, from observations to simulations, suggests that warmer climates lead to more intense precipitation events even in regions where the total annual precipitation is reduced slightly, and with the possibility for correspondingly larger increases in intensity where the total amount of precipitation also increases (Solomon et al. 2007). This is meaningful since extremes in precipitation arguably matter more than the mean for erosion and natural hazards, such as floods and landslides. From a geological and land surface processes perspective, interesting questions thus arise concerning the sensitivity of erosion to changes in precipitation intensity.

We seek to understand how dynamical changes in the hydrological cycle affect the statisti-

cal distribution of precipitation. A natural starting point, and the inspiration for the present study, is to understand how large-scale atmospheric circulation patterns control the shape of the daily precipitation distribution in the modern record. An observational analysis also provides a target for model evaluation. Our approach is to consider the natural variability of the precipitation response in the American West attributed to El Niño Southern Oscillation (ENSO). ENSO is generally considered to be the dominant pattern of global interannual climate variability. It is associated with hemisphere-wide precipitation and temperature anomalies that are consistent with a meridional shift in the position of the midlatitude tropospheric jet and Pacific storm track. Wintertime precipitation anomalies associated with ENSO have been extensively discussed in the scientific literature, and numerous studies have demonstrated enhanced seasonal precipitation in the southwest and suppressed precipitation in the northwest during El Niño events, and vice versa during La Niña (e.g. Mo and Higgins 1998; Schonher and Nicholson 1989; Kahya and Dracup 1994; Dettinger et al. 1998). Hence it is clear that ENSO in the American West is a natural setting for probing further into the dynamical controls on large-scale precipitation patterns.

Wintertime daily statistics follow the general theme of seasonal precipitation, with enhanced daily precipitation expected in the southwest during El Niño and the northwest during La Niña. The importance of understanding the shape of the statistical distribution of precipitation, and the manner by which changes in mean translate into probabilities of extreme events, has been noted in other studies, but with emphasis ultimately placed on the higher percentiles rather than the full distribution. For example, Higgins et al. (2007, 2008) demonstrate wintertime increases in the mean frequency of daily precipitation and in the amount of accumulated precipitation from heavy events (greater than 90th percentile) in

the southwest during El Niño and the northwest during La Niña. In addition, Cayan et al. (1999) find increases during El Niño in the frequency of heavy precipitation days (greater than 50th and 90th percentile) and an amplified and lagged streamflow response in the southwest, and likewise during La Niña in the northwest. Similar patterns in precipitation are also observed for the frequency of greater then 75th percentile events, for ENSO relative to the climatological mean (Gershunov and Barnett 1998; Gershunov 1998).

An alternate to comparing the means and extremes of precipitation is to evaluate the shape of the full statistical distribution of precipitation. For example, Sardeshmukh et al. (2000) apply statistical tests to identify regions (globally) of changes in the shape of the seasonal mean precipitation distribution for ENSO winters, using GCM ensembles and monthly observations. The authors also identify regions of changes in the probability of extreme values, and evaluate whether these changes are due to shifts in the mean or changes in shape. They find that along the Pacific Coast of North America, changes in the shape of seasonal precipitation indeed occur during ENSO events, and in turn affect the probability of extreme events. By evaluating the shape of daily wintertime precipitation during ENSO events, our study effectively fills the gap between a global shape analysis of the seasonal distribution of precipitation (e.g. Sardeshmukh et al. 2000), and a consideration of only the higher percentile ranks for regional daily precipitation (e.g. Cayan et al. 1999). In the same vein, a recent study by Becker et al. (2009) analyzes the effect of ENSO on the parameters of a theoretical distribution function fit to daily rainfall.

ENSO is also of interest because its associated precipitation anomaly pattern in the American West straddles the dry subtropical zone of the Desert Southwest and wet midlatitude zone of the Pacific Northwest. These zones are projected to have different precipitation

responses under global warming scenarios, hence defining a border region of high sensitivity to a changing climate. It is also important to remember that the response of ENSO itself to a warmer climate is by no means clear. Whereas mean tropical Pacific SST are expected to shift towards more 'El Niño-like' conditions in a warmer climate (with no agreement on change in interannual variability or event amplitude) (van Oldenborgh et al. 2005; Solomon et al. 2007), the zonal mean atmospheric circulation response to global warming suggests a weakening and expansion of the Hadley Cell and poleward shift of the midlatitude jet, consistent with La Niña, rather than El Niño, processes (Lu et al. 2008; Chen et al. 2008). Given these apparently conflicting responses, we emphasize that we do not consider ENSO to be an analog for the future climate. Rather we are concerned with how a rearrangement of the patterns of heating and circulation in the atmosphere influences the statistical distribution of precipitation, and we recognize that understanding these processes may have implications for projections of future climate. In addition, while any of the many identified modes of atmospheric circulation could be used to investigate the natural variability of the precipitation distribution, we choose ENSO in the western U.S. as a natural case study with large societal impacts. However the same analysis framework can be readily applied to any mode of natural variability.

2. Data, Methods, and the Meaning of 'Wetter'

We use the CPC Unified Rain Gauge Database (URD) of gridded (0.25° x 0.25°) daily station data for 1948-1998 (Higgins et al. 2000) to evaluate wintertime (defined here as November through March, or NDJFM) precipitation in the American West as a function

of ENSO. On a typical day the URD includes ∼13,000-15,000 reporting stations across the United States. We choose the URD because it represents the best-available source of daily, high-resolution, multidecadal, and station-based precipitation data for the region. Statistical significance of differences in the mean and shape of daily precipitation distributions are evaluated for El Niño relative to La Niña winters. Strong ENSO events are selected based on whether the wintertime mean SST anomaly within the Niño 3.4 region in the tropical Pacific (5°N-5°S, 170-120°W) (Trenberth 1997) exceeds a threshold of ±1K (Table 1). No statistical comparison is made to the mean state or neutral ENSO years, although inspection of mean-state ENSO conditions (not shown) confirms that the precipitation distribution lies between that of strong El Niño and La Niña winters.

Figure 1 shows the wintertime-mean daily precipitation time series averaged over the southwest (SW) and northwest (NW) regions (30.5-40°N, 110-126.25°W and 40-49.5°N, 110-126.25°W, respectively). These regions are selected because they exhibit coherent spatial precipitation patterns during ENSO events. In addition, we halved the region to consider only precipitation west of 116°W and found results to be consistent. Several features are striking from this figure. First, according to the Student's t statistic, there is no trend in the precipitation time series at the 5% significance level in either region (allowing for only a 5% chance of incorrectly rejecting the null hypothesis). We note that, for the whole of the United States and over the full twentieth century, other studies have identified significant trends (Groisman et al. 2004). However the important point here is that any trend at the regional level in our data is swamped by the interannual variability. Hence we are not concerned with a sampling bias with respect to the selected ENSO years, which might arise from the predominance of strong La Niñas in the early half of the record and strong El

Niños in the latter half. Secondly, the time series serves as an excellent reminder that the ENSO phenomenon only explains some of the precipitation variability in the western U.S. Not all wet years are strong ENSO years, and there exists quite a bit of scatter in the amount of precipitation during strong ENSO events. However overall we see that in the SW the wintertime mean precipitation averaged over El Niño winters is greater than during La Niña winters, whereas in the NW the wintertime mean precipitation is greater during La Niña, consistent with the canonical picture of wintertime ENSO precipitation impacts in the American West. This is confirmed in statistical tests presented in the next section.

It is also necessary to carefully define what is meant by 'wetter' or 'drier', as there are several different ways of characterizing changes in precipitation. Figure 2a shows the density distribution of daily precipitation averaged over the NW, and Figure 2b shows the same information represented as a cumulative distribution. Broadly speaking we might imagine a shift in the mean of the statistical distribution of precipitation (the mean is indicated by the dashed lines in Figure 2), or a change in the shape of the distribution. In addition, changes in the precipitation distribution may be described by a change in the frequency of precipitation events or in the amount of rain per event. In other words, a wetter climate may be one in which precipitation either occurs more often or is more intense, or a combination of both. When considering the latter, we weight the frequency of events by the amount of precipitation per event, such that the distribution, when plotted, gives the fraction of total rain as a function of daily rainfall rate (Figure 2c). The histogram of the weighted case de-emphasizes the drizzle and emphasizes the heavy precipitation events in the tail of the distribution (compare Figures 2b and c).

It is easy to appreciate that for a small (or even no) shift in the mean precipitation,

there is the possibility for a large change in the contribution from intense events to the precipitation total. For example, previous studies have used the two-parameter gamma distribution to model daily precipitation amounts and have demonstrated that modest changes in mean precipitation tend to be accomplished by a larger proportion derived from heavy rainfall events (Groisman et al. 1999; Wilby and Wigley 2002; Becker et al. 2009). This is attributed to changes in the scale parameter, which essentially controls the spread of the gamma distribution. We choose to characterize the general shape of the daily precipitation data, rather than fitting it to the parameters of a theoretical function such as the gamma distribution. While the gamma function is an efficient descriptor and facilitates comparison of distributions, the value of our approach is that it allows for complete characterization of changes in the distribution and, in addition, avoids possibly underfitting the data with a prescribed mathematical function.

3. Analysis

Distributions of daily precipitation during El Niño and La Niña winters are evaluated and compared using two standard statistical tests, the two-sample t test for mean and the nonparametric Kolmogorov-Smirnov (K-S) test for distribution shape (Massey 1951; Stephens 1979). Statistical significance is established by allowing for only a 5% chance of incorrectly rejecting the null hypothesis ($\alpha = 0.05$). The null hypothesis states that the means or shapes of El Niño and La Niña precipitation are equal for the t test and K-S test, respectively. The t test in principle involves two assumptions: normality and data independence. Daily precipitation, however, has a highly skewed distribution and exhibits

large day-to-day correlation. As elegantly shown by Boneau (1960), the t test is functionally robust to non-Gaussian distributions, particularly for large sample sizes. This is true even for the extreme case of the exponential distribution. The second assumption of serial correlation we correct for, as described in Sections a1 and b1.

In regards to the K-S test, it is noteworthy that - because the distributions are *cumulative* - once a significant separation occurs anywhere between the distributions, then the null hypothesis is rejected and the distributions are statistically different, regardless of the behavior elsewhere within the distributions. The K-S test searches for the maximum in the vertical separation between two cumulative distributions, $f(x)$ and $g(x)$, given by

$$D_{ks} = max(|f(x) - g(x)|), \tag{1}$$

and determines based on this spread whether the data are from the same or different distributions. In the analyses that follow, we evaluate both the spatial patterns of mean precipitation as a function of ENSO (Section a), as well as the shape of the precipitation distributions in regional averages (Section b). Absolute changes in extreme precipitation are discussed in Section c. In particular, we focus on the southwest (SW) and the northwest (NW) regions of the American West, as defined in Section 2.

a. Change in mean

We begin by evaluating how mean daily wintertime precipitation varies with ENSO phase, and address the canonical picture of ENSO precipitation impacts (e.g. Mo and Higgins 1998;

Schonher and Nicholson 1989; Kahya and Dracup 1994; Dettinger et al. 1998). Figure 3 shows mean daily wintertime precipitation when raining, or mean daily intensity, in the study region for El Niño minus La Niña events. We hereafter refer to El Niño as warm ENSO events and La Niña as cold ENSO events. Across the western U.S. we find that, when raining, the maximum difference between daily rainfall rates in warm and cold ENSO events is more than 3 mm/day (Figure 3a). As in the regional average (Figure 1), this variability is sufficiently large with respect to observed or projected trends that we can be confident our analysis is not polluted by sampling biases. In addition, there is an increase in mean daily precipitation intensity in the SW during warm events (up to 87%), in the NW during cold events (up to 56%), and a striking nodal line in the differenced precipitation field at roughly 40°N, indicating a zone of little-to-no change in mean intensity associated with ENSO (Figure 3b). Overall there is a clear difference in mean daily precipitation intensity during warm and cold ENSO events, and these features are generally consistent with previous studies of ENSO precipitation impacts as discussed in Section 1.

We now evaluate the statistical significance of these observations, and in Section b identify how changes in mean are accomplished by changes in the frequency and intensity of precipitation. A discussion of how degrees of freedom were estimated in attributing significance follows at the end of this section. Applying the t test to each grid cell reveals a widespread pattern of statistically-significant increases in mean (i.e. averaged across all days) daily intensity during warm (cold) events across the SW (NW) relative to cold (warm) events at the 5% significance level (Figure 4), confirming the canonical picture of ENSO precipitation impacts in the mean. In addition, applying a more rigorous significance level (e.g. 1%) has only a minimal effect on the spatial pattern of statistical significance. This

increase in mean daily precipitation intensity appears to be a robust result and is supported by several lines of evidence: It is evident in the spatial maps of observed precipitation differences and confirmed by t tests applied at the grid cell level. It is also supported by t tests applied to the NW and SW aggregate data (Section c), providing a consistent story in all cases tested.

There are also interesting regional variations in the effect of ENSO phase on precipitation. In particular we consider a range of precipitation thresholds in order to understand the frequency signal as a function of daily rainfall rate. For example, we find that the frequency of drizzle in the NW is relatively unaffected by cold ENSO events. Figure 3c shows that changes in the fractional number of rainy days are small across much of the NW (less than 10%), whereas in considering only precipitation $\geq$5 mm/day, there is a much more obvious increase in the fractional number of rainy days during warm events in the SW and cold events in the NW, particularly along the coast (Figure 3d). This suggests that in the NW the total number of rainy days is dominated by drizzle and is less sensitive to ENSO phase, consistent with the finding by Cayan et al. (1999) that the fractional increase in precipitation frequency associated with ENSO is larger in the SW than the NW. Applying the t test, after correcting for spatial and temporal correlation, to the frequency of precipitation events (not shown) reveals an increase in the mean number of rainy days during warm events in the SW *and* in the NW at the 5% significance level. This is evidenced in Figure 3c by the northward of 40°N extension of increases in warm event precipitation frequency. If even a 1 mm/day precipitation threshold is imposed (ignoring all precipitation <1 mm/day, and thereby removing the drizzle effect) we do indeed see a significant increase in the number of rainy days in the NW during cold events. This result holds true for every precipitation

threshold greater than and including 1 mm/day.

1) Adjustment for temporal correlation of data

Serial correlation arises as an issue when applying the t test to climatological data, and we detour briefly to discuss this here. The conventional t test assumes statistically independent data, which is generally not the case for daily precipitation. The effect of serial correlation is that the test will too frequently return a significant difference in means where no difference exists. In other words, the actual significance level is higher than the specified significance level. This behavior is occasionally referred to as liberal, to differentiate it from a conservative test. A standard approach is to compute the effective degrees of freedom, sometimes referred to as the equivalent sample size in time series analysis. The ensuing reduction in degrees of freedom accounts for the information loss due to serial correlation. We apply this technique throughout our analysis, after von Storch and Zwiers (1999), by calculating the decorrelation time and effective degrees of freedom at each grid cell from wintertime climatology. On average, this amounts to a 10% reduction in the degrees of freedom. In Section c we extend this treatment to account for effective spatial degrees of freedom as well.

b. Change in shape

We now focus in more detail on how the shape of the precipitation distribution changes as a function of ENSO phase. We apply the K-S test to identify differences in the shape of the distributions between warm and cold events, both in terms of the fraction of rainy days

and the fraction of total rain amount. These analyses illuminate how the changes in mean precipitation shown in the previous section are accomplished by changes in the frequency or intensity of precipitation. In order to evaluate fractional differences in the amount of precipitation, we weight the distributions by the daily rainfall rate as discussed in Section 2.

Figures 5a and b show the spatial patterns of the K-S test applied to the distributions of the fraction of rainy days as a function of daily rainfall rate. The geographic regions of statistical significance correspond well with those identified in the previous section for changes in mean daily intensity according to the t test (Figure 4). However when the K-S test is applied to the weighted distributions representing the fraction of total rain, there are notable differences. In particular, the pattern of significance becomes less regionally-concentrated and more diffuse. Figure 5c shows that a shift in the weighted precipitation distribution towards more intense daily rainfall rates during warm events is still largely confined to the SW. In contrast, in Figure 5d we see that a significant shift in the weighted distribution towards more intense precipitation occurs across an extended region of the western U.S. during cold events. Recalling the cumulative nature of the test, it is important to emphasize that these maps are best interpreted as providing a geographic overview of where the shapes of the distributions differ, rather than indicating the relative importance of cold or warm events for a particular rainfall rate. Interestingly, Figure 5d hints at an influence of cold-event weather systems that extends farther south than expected. This topic is addressed in detail in Feldl and Roe (2010).

The coherent spatial patterns evident in Figure 3 lead us to consider daily regional averages of the precipitation data, where raining. Given this approach, the area over which we average may change depending on the number of rainy grid cells. The regional averages

consist of 1120 cold-event rainy days and 1209 warm-event rainy days. We first focus on the cumulative distributions of daily precipitation frequency for warm and cold events. The nature of the K-S test effectively normalizes the distributions, and ensures that the influence of ENSO on the frequency of precipitation is not obscured by the differing amounts of total seasonal precipitation in our two regions. Figures 6a and b present a comparison of the cumulative distributions of regionally-averaged daily precipitation frequency for warm and cold events in the SW and NW, respectively. We conclude from the K-S test that the shapes of the distributions are indeed statistically different, and moreover we find a significant increase in the fraction of total rainy days that are heavy rainy days (hereafter, heavy rainy day fraction) during warm (cold) relative to cold (warm) events in the SW (NW). This result is apparent from a shift in the warm event distribution towards more intense daily rainfall rates in the SW, and likewise for cold events NW.

This and subsequent results are based on interpretation of the cumulative distributions and hence a brief discussion is warranted. Focusing on Figure 6a for the SW, a shift in the warm event distribution towards the right implies that for every daily rainfall rate, the warm event distribution has achieved a smaller percentile of its total rainy days than the cold event distribution, which means a larger fraction is available to occur at more intense daily rainfall rates (i.e., imagine taking a vertical slice through the distributions). This shift is accompanied by an increase in mean daily precipitation intensity (as indicated by the dashed lines) during warm events in the SW, once again corroborating the robustness of our t test result in the mean on both a grid cell level (Figure 4) and in the regional mean. An alternate perspective follows that for every percentile rank, the warm event distribution occurs at a higher daily rainfall rate than the cold event distribution (imagine a horizontal slice). For

example, 10% of all rainy days (greater than 90th percentile) occur at regionally-averaged rainfall rates of greater than 6.3 mm/day for warm events and greater than 4.9 mm/day for cold events in the SW. Similarly in the NW (Figure 6b), 10% of all rainy days occur at regionally-averaged rainfall rates of greater than 6.2 mm/day for warm events and 7.0 mm/day for cold events.

In these plots the gray shading centered on the warm-event distribution represents the 95% confidence limits ($100 \times (1 - \alpha)$, where α is the significance level). If the cold-event distribution lies anywhere outside this gray envelope, then we may conclude, with 95% confidence, that the distributions are statistically different by the K-S test. Due to the integrative nature of cumulative distributions, which must converge at the upper and lower limits, the distributions are required to be contained within the 95% confidence interval at the highest and lowest rainfall rates. In other words, it is important not to construe that the distributions differ only at the rainfall rates where a separation is observed, and in fact differences may occur in the tails. Separation of the cumulative distributions at any given daily rainfall rate simply means that differences across all rainfall rates up to that point have accumulated to become statistically significant. Values of the K-S test statistic D_{ks} are given in Table 2. Recall the test statistic indicates the maximum separation between the cumulative distributions and is the metric for distinguishing whether the warm and cold event precipitation distributions are statistically different.

Turning now to the weighted case, a statistically-significant change in shape due to an increase in the fraction of total rain contributed by heavy precipitation (hereafter, heavy rain fraction) is observed during warm relative to cold events in the SW (Figure 6c), and during cold relative to warm events in the NW (Figure 6d). Hence when considering the full

distributions, we find both increases in the frequency and intensity of heavy precipitation in the SW during warm events and in the NW during cold events. This result is consistent with previous work (e.g. Higgins et al. 2007; Cayan et al. 1999). In addition, a recent study by Becker et al. (2009) finds that the Southwest is scale-dominated during warm events (referring to the scale parameter of the gamma distribution), which the authors interpret as an increase in the relative frequency of intense precipitation days.

Figure 6c further hints at an intriguing result: At the very highest rainfall rates in the SW (greater than 99th percentile), the heavy rain fraction from cold events actually exceeds that from warm events. That is, the daily rainfall rates for the top 1% of precipitation are higher during La Niña than during El Niño in the SW. Note that this is in line with our expectation that shifts in the cold-event distribution towards more intense daily rainfall rates are widespread across much of the American West and not limited to the NW (Figure 5d). We cannot conclude as to the significance of this result directly from the cumulative distributions, and instead we apply a different technique in Section c to search for significance in the tail of the distributions.

The comparison of the distributions for frequency and intensity presented in this section supports our earlier conclusion that the precipitation response is nuanced and dependent on the particular question being asked. In what follows, we explore this idea further by identifying changes in the shape of the precipitation distributions independent of shifts in the mean. Namely, we normalize the x axis for each distribution such that a value of one equals the mean daily rainfall rate (and a value of two is twice the mean daily rainfall rate). One benefit of this approach is that it allows one to compare the 'flashiness' of the distribution, or in other words the probability of extreme excursions far from the mean.

Figure 7 shows the adjusted cumulative distributions of warm and cold event precipitation in the SW and NW. We find no significant change in the frequency distribution of rainy days relative to the mean in the NW (Figure 7b). This is not surprising given our earlier result showing that the frequency of drizzle in the NW is relatively unaffected by ENSO state and tends to damp the frequency response in the full distribution. In the SW there is a small but significant departure between the distributions, suggesting (1) an increase in the fraction of rainy days that are moderate rainy days during warm events and (2) an increase in the heavy rainy day fraction (greater than 87th percentile) during cold events (Figure 7a). This redistribution of the number of rainy days is indicated by the intersection of the distributions near twice the mean daily rainfall rate.

Figures 7c and d allow us to characterize the 'flashiness' of the precipitation, or how closely the distribution clusters near the mean. We see a statistically-significant increase in the fraction of total rain contributed by above-mean events during cold (warm) relative to warm (cold) events in the SW (NW). In other words, during warm events in the SW the distribution is steeper at moderate rainfall rates, indicating that a larger portion of the precipitation distribution clusters near the mean daily regional-mean intensity. In contrast, precipitation is flashier (has a lower kurtosis) during cold events in the SW. Combining the results for the SW from Figures 6c and 7c, we find an increase for warm events in the heavy rain fraction (in an absolute, mm/day sense), but also an increase in the kurtosis, or a narrowing of the distribution.

Several additional points are striking and worth emphasizing. In the SW we see significant changes in both the frequency of events (albeit small) and intensity of precipitation relative to the mean, whereas in the NW only changes in intensity are significant. In other words,

there do not appear to be significant changes in the relative distribution of the number of rainy days between warm and cold events in the NW. Secondly, these results demonstrate a fundamental difference in the shape of the weighted distributions independent of shifts in the mean during warm and cold events. The differences between warm and cold events cannot simply be explained by a shift in the mean daily intensity, but rather an actual redistribution of the relative proportions of regional-mean precipitation is necessary.

Finally in all cases we see that the increases in the fraction of total rain contributed by the heaviest precipitation occurs during cold events rather than warm events (Figures 6c-d and 7c-d). This is true for both geographic regions. However we emphasize that this result is specific to the intensity of heavy precipitation only. When the the full range of precipitation is considered, as is clear from several figures, mean El Nino precipitation still exceeds La Nina in the SW. In the next section, we further explore the intense cold-event precipitation signal inferred from the tails of the distributions.

c. Change in extremes

Cumulative distributions of total rainfall amount suggest that the intensity for the top 1% of precipitation events is enhanced during La Niña relative to El Niño in the SW regional average. This finding is particularly relevant to weather extremes and their associated impacts. What strategies can we use to evaluate the tails of the distributions statistically? Our preferred approach is to consider only the individual heavy precipitation events, and to search for the local rainfall threshold above which cold events demonstrate an increased mean according to the t test. This picks out the intense but possibly isolated events, and

does not necessarily speak to a regional picture. On the other hand, it is relevant to local and damaging severe-weather phenomena such as landslides and flash floods.

As a brief aside, a second approach is to focus on all precipitation concurrent with heavy events, in essence, applying a regional-mean threshold. With this approach we find that, as suggested by the tail of the cumulative distributions in Figure 6c, for regional-mean thresholds of at least 11 mm/day cold events demonstrate an increase in mean daily regional-mean intensity in the SW. Recalling from Section b that the average is taken over rainy grid cells only, these regional means represent extraordinarily high rainfall rates, and only a handful of events exist for regional-mean precipitation $\geq$11 mm/day. As such, there is not enough statistical power to declare significance. Hence we conclude that this result is more of a curiosity than a convincing climatic signal.

Returning to the local threshold analysis, we construct an aggregate data set for each threshold, without prior averaging. Thus each precipitation event represents a single time and place. The t test is then applied to search for differences in mean daily rainfall rate for the thresholded data. A drawback of the above-mentioned regional threshold analysis is that, because it is the averaged data (again, only over rainy cells) to which the threshold is applied, one rainy grid cell on an otherwise dry day will have as much of an effect as one thousand rainy grid cells during a widespread precipitation event. This effect is particularly troublesome at high thresholds where precipitation is sparse. In contrast, in using the local threshold and aggregate data set, a widespread dry day will contribute few rain events, and a widespread rainy day will contribute many events. Precipitation is in essence weighted by the spatial extent of the storm, simply by nature of the aggregate. An additional benefit of this technique is that we retain more data, hence increasing the statistical power of the test

to obtain significant results. For instance, for no threshold, we have over two million pooled precipitation events across the SW region, decreasing to 1671 for a 70 mm/day threshold. Likewise for the NW, over four million, decreasing to 3159.

Figure 8 shows the difference in mean precipitation rate as a function of threshold for the SW and NW. A discussion of how degrees of freedom were estimated for the regional aggregate follows at the end of this section. As must be the case from prior analysis, for no threshold applied (i.e. 0 mm/day threshold), mean daily precipitation is significantly increased during warm relative to cold ENSO events in the SW, and vice versa in the NW. In addition, for all thresholds considered the NW conforms to the expected picture, with cold-event precipitation increased over warm-event precipitation (Figure 8a). However beyond thresholds of 6 mm/day, the spread between means is not large enough to be assessed as significant. In stark contrast is the signal in the SW (Figure 8b). As the threshold is raised to even 1 mm/day, the result that warm-event precipitation is greater than cold-event precipitation falls below the 95% confidence level. And for thresholds exceeding about 20 mm/day, we instead find that mean precipitation rates during cold events actually exceed those during warm events. The mean of the aggregate precipitation given a 20 mm/day threshold represents the $\sim$99th percentile rainfall rate. The synoptic conditions associated with these intense local precipitation events in the SW are explored in Feldl and Roe (2010). In summary, in both regions precipitation follows the canonical picture of increases in the SW during El Niño and in the NW during La Niña when considering the full range of precipitation, whereas for intense precipitation, rainfall rates in the SW are in fact higher during La Niña.

We emphasize that our result is an intensity signal not a frequency signal, and there

is no significant increase in the number of rainy days during cold events in the SW for precipitation $\geq$20 mm/day (see appendix for further detail). *Rather we find that while heavy precipitation in the SW is more intense during cold events, it is more frequent during warm events.* In other words our results suggest that, for the SW, La Niña winters experience more locally intense precipitation (relevant to landslide hazards), whereas El Niño winters experience enhanced precipitation across the entire region and more frequent heavy rains (relevant to reservoir management). Localized regions of significant increases in mean daily intensity during warm ENSO events persist over the Southern Coast Ranges of California for thresholded precipitation but do not survive spatial averaging.

1) Adjustment for spatial correlation of data

As discussed earlier, applying the t test to daily precipitation, which is correlated in both time and space, requires an adjustment accounting for data dependencies. In Figure 8 we use a bracketing approach to constrain the upper and lower limits on the effective degrees of freedom, and translate these bounds into the acceptable range of spread allowed by the t test. Note that as the threshold is raised to include increasingly extreme events, we lose observations and hence degrees of freedom (as indicated by the widening of the confidence intervals). Likewise, we also lose degrees of freedom by correcting for serial correlation. The lower bound (dashed line in Figure 8) is obtained by assuming perfect spatial correlation, or in other words, one degree of freedom per day, and then reducing this further to account for temporal correlation following our method in Section a. The upper bound (gray envelope) is obtained by calculating the effective spatial degrees of freedom from the precipitation

data ($N^*_{ef} \sim 3.5$) after Bretherton et al. (1999) - which explicitly considers non-Gaussian precipitation data - and multiplying this by our lower bound. Due to assumptions inherent in the adjustment, this may still represent an overestimate of the actual degrees of freedom.

4. Discussion and Conclusions

In this study we characterized how the daily distribution of precipitation is linked to a major mode of climate variability. Using ENSO as a case study for changes in midlatitude circulation patterns, we evaluated 50 years of wintertime precipitation during El Niño and La Niña winters in the American West, based on a comprehensive, high-resolution, station-based dataset. Our major results are as follows:

- Increase in mean daily precipitation intensity is confirmed across the SW during warm ENSO events and across the NW during cold ENSO events.

- Change in mean is accomplished by a shift in the distributions of daily precipitation frequency and amount towards more intense daily rainfall rates.

- Frequency of drizzle (<1 mm/day) in the NW is largely unaffected by ENSO state.

- Fundamental changes in the shape of the precipitation distributions are observed, independent of shifts in the mean.

- For heavy precipitation, cold events show an increase in mean daily intensity across the SW.

For all cases applied to the full range of daily rainfall rates in the SW, we find that both local and regional-mean precipitation is larger during warm than cold ENSO events. However in considering extreme precipitation, cold ENSO events demonstrate a significant increase in mean daily intensity when aggregated over the entire region. In map view, the spatial pattern of intense cold-event precipitation is diffuse (Figure 9a). We find that approximately half of all the grid cells that experience intense ($\geq$20 mm/day) precipitation in the SW region show an increase in mean cold-event precipitation over warm-event precipitation. However less than 1% of the intensely-precipitating grid cells in the SW have sufficient number of temporally-uncorrelated observations to distinguish statistically between warm and cold ENSO means. This speaks to our earlier point, and provides motivation for using the regional aggregate. As the threshold is raised to consider increasingly extreme precipitation, we lose degrees of freedom and statistical power. As a result, the statistics are severely hampered at the grid cell level, whereas in the regional aggregate we retain adequate information to address the extremes statistically.

The richness of the spatial pattern emphasizes one of the strengths of our analysis, that by considering both regional and local effects, we gain a deeper understanding of how patterns of climate variability affect precipitation. The diffuse pattern of intense precipitation is expected due to the well-known low degree of spatial correlation in precipitation, compared to other climatological variables. In addition, we have already remarked on the high variability evidenced in the time series of regionally-averaged ENSO precipitation (Figure 1). Not only is it true that not all strong warm-event years are wet in the SW, but conversely we see that some strong *cold* events are in fact very wet in the SW. Finally, we also note that the western U.S. is characterized by complex topography, including two major north-south

oriented mountain ranges. Local and orographic effects are expected to lead to enhanced spatial variability across the region.

We find that distinct perspectives are gained by evaluating both the spatial patterns and regional aggregates of precipitation differences. Figure 9 shows the spatial extent of wintertime differences in the intensity and frequency of heavy precipitation that comprise the regional-mean picture. That intense cold-event precipitation matters on a local scale across the SW is indicated by the diffuse spatial pattern, combined with the significant increase for the region as a whole. From composite analysis of several climate variables, these intense cold-event precipitation days in the southwest arise from the presence of a persistent offshore trough, and the simultaneous emplacement of a strong source of subtropical water vapor (Feldl and Roe 2010). While La Niña winters experience more locally intense precipitation in the SW, El Niño winters experience enhanced regional-mean precipitation and more frequent heavy rains (Figure 9b). Thus depending on the impact of interest, be it landslides or reservoir management, either El Nino or La Nina conditions may have the stronger signal. In addition, we can identify from Figure 9 areas of southern California that are particularly sensitive to El Niño in that they exhibit increased intensity *and* frequency of heavy precipitation during warm events.

Our goal in this study was to investigate the link between large-scale atmospheric circulation and daily precipitation statistics, in the context of our two climatic regions, the northwest and southwest of the western U.S. While for most metrics the choice of the 40°N demarcation between climate zones is a good approximation to the patterns of precipitation variability, there are two notable exceptions. First, that El Niño weather influences the NW in the frequency of drizzle (<1 mm/day) (Figure 3c), and secondly that La Niña weather

influences the SW in the intensity of heavy precipitation ($\geq$20 mm/day) (Figure 9a). We speculate that this observation may represent a difference in character between the northward extension of drizzly warm-front preciptiation and the southward extension of intense cold-front precipitation. The main lesson here is that we cannot simply describe the response to changing patterns of circulation as a shift in the climatic zones, but that a more nuanced view is necessary, at least when considering the full spectrum of precipitation.

An abiding theme of this analysis is that extreme local events do not have to behave according to the regional mean. This point illustrates important subtleties in regional-scale climate predictability. It is interesting to consider whether the details of the daily precipitation distribution provide a benchmark for establishing confidence in climate prediction (e.g. Allan and Soden 2008). It seems a natural requirement that models have skill in reproducing observed precipitation statistics, particularly for impacts-related projections of extreme precipitation. More broadly speaking, how well do we have to understand the SST and circulation forcings in order to have skill in predicting the precipitation response for a given climate, be it past, modern, or future? Some studies have employed statistical-dynamical methods towards this end (e.g. Gershunov and Cayan 2003). That we have found important differences depending on whether one considers frequency, intensity, or extremes suggests that it may be worthwhile to revisit the shape of the precipitation distribution for other circulation regimes - in addition to the midlatitude and largely maritime scenario presented here. Such considerations are highly relevant to the weather experienced under a changing climate.

Acknowledgments.

We thank Lynn McMurdie and Chris Bretherton for insightful conversations. We are also grateful to three anonymous reviewers for thorough and constructive comments, and to editor Anthony Del Genio. This work was supported by the National Science Foundation (EAR-0642835).

APPENDIX

Changes in intensity for thresholded precipitation

Mathematically, the relationship between frequency and intensity of thresholded precipitation is represented by

$$\overline{p}_{p_i \geq p^*} = \frac{\sum_{i>i^*}^{\infty} n_i p_i}{\sum_{i>i^*}^{\infty} n_i},$$

in which the mean intensity $\overline{p}$ over a threshold p^* is given by the total amount of precipitation divided by the total number of aggregate precipitation events over that threshold. For an increase in intensity ($\overline{p}$) to occur, there must be a redistribution of precipitation events (n_i) towards more intense rainfall rates (p_i), such that the total amount of precipitation is increased.

Figure A1a shows the aggregate number of rainy days as a function of precipitation threshold for the southwest (the northwest results are shown in the inset figure). The frequency of rainy days is always greater during warm than cold ENSO events, although at high thresholds the frequency distributions converge. When the data are plotted as a fraction of rainy days (Figure A1b) the curves intersect, such that at high thresholds ($\geq$40 mm/day) cold events contribute a larger fraction of rainy days relative to warm events. Strikingly, this redistribution does not occur in the northwest (as seen in the inset). In other words, the increase in the intensity of heavy precipitation during cold ENSO events requires that, at some higher threshold, the proportion of rainy days that occur at intense rainfall rates

must also increase. Figure A1 is a clear way of showing the redistribution of precipitation events that explains the results in Section 3c.

REFERENCES

Allan, R. P. and B. J. Soden, 2007: Large discrepancies between observed and simulated precipitation trends in the ascending and descending branches of the tropical circulation. *Geophysical Research Letters*, **34**.

Allan, R. P. and B. J. Soden, 2008: Atmospheric Warming and the Amplification of Precipitation Extremes. *Science*, **321**, 1481–1484.

Allen, M. R. and W. J. Ingram, 2002: Constraints on future changes in climate and the hydrological cycle. *Nature*, **419**, 224–232.

Becker, E. J., E. H. Berbery, and R. W. Higgins, 2009: Understanding the Characteristics of Daily Precipitation Over the United States Using the North American Regional Reanalysis. *Journal of Climate*, **22**, 6268–6285.

Boneau, C. A., 1960: The effects of violations of assumptions underlying the t test. *Psychological Bulletin*, **57 (1)**, 49–64.

Bretherton, C. S., M. Widmann, V. P. Dymnikov, J. M. Wallace, and I. Bladé, 1999: The Effective Number of Spatial Degrees of Freedom of a Time-Varying Field. *Journal of Climate*, **12**, 1990–2009.

Cayan, D. R., K. T. Redmond, and L. G. Riddle, 1999: ENSO and Hydrologic Extremes in the Western United States. *Journal of Climate*, **12**, 2881–2893.

Chen, G., J. Lu, and D. M. W. Frierson, 2008: Phase Speed Spectra and the Latitude of Surface Westerlies: Interannual Variability and Global Warming Trend. *Journal of Climate*, **21**, 5942–5959.

Dettinger, M. D., D. R. Cayan, H. F. Diaz, and D. M. Meko, 1998: North-South Precipitation Patterns in Western North America on Interannual-to-Decadal Timescales. *Journal of Climate*, **11**, 3095–3111.

Feldl, N. and G. H. Roe, 2010: Synoptic weather patterns associated with intense La Niña precipitation in the southwestern United States. *Geophysical Research Letters*, in review.

Gershunov, A., 1998: ENSO Influence on Intraseasonal Extreme Rainfall and Temperature Frequencies in the Contiguous United States: Implications for Long-Range Predictability. *Journal of Climate*, **11**, 3192–3203.

Gershunov, A. and T. P. Barnett, 1998: ENSO Influence on Intraseasonal Extreme Rainfall and Temperature Frequencies in the Contiguous United States: Observations and Model Results. *Journal of Climate*, **11**, 1575–1586.

Gershunov, A. and D. R. Cayan, 2003: Heavy Daily Precipitation Frequency over the Contiguous United States: Sources of Climatic Variability and Seasonal Predictability. *Journal of Climate*, **16**, 2752–2765.

Groisman, P. Y., R. W. Knight, T. R. Karl, D. R. Easterling, B. Sun, and J. H. Lawrimore, 2004: Contemporary Changes in the Hydrological Cycle over the Contiguous United States: Trends Derived from In Situ Observations. *Journal of Hydrometeorology*, **5**, 64–85.

Groisman, P. Y., et al., 1999: Changes in the probability of heavy precipitation: Important indicators of climatic change. *Climatic Change*, **42**, 243–283.

Held, I. M. and B. J. Soden, 2006: Robust Responses of the Hydrological Cycle to Global Warming. *Journal of Climate*, **19**, 5686–5699.

Higgins, R. W., W. Shi, E. Yarosh, and R. Joyce, 2000: Improved United States precipitation quality control system and analysis, NCEP/Climate Prediction Center ATLAS No. 7. Tech. rep., National Oceanic and Atmospheric Administration, 40 pp.

Higgins, R. W., V. B. S. Silva, V. E. Kousky, and W. Shi, 2008: Comparison of Daily Precipitation Statistics for the United States in Observations and in the NCEP Climate Forecast System. *Journal of Climate*, **21**, 5993–6014.

Higgins, R. W., V. B. S. Silva, W. Shi, and J. Larson, 2007: Relationships between Climate Variability and Fluctuations in Daily Precipitation over the United States. *Journal of Climate*, **20**, 3561–3579.

Kahya, E. and J. A. Dracup, 1994: The Influences of Type 1 El Niño and La Niña Events on Streamflows in the Pacific Southwest of the United States. *Journal of Climate*, **7**, 965–976.

Kharin, V. V., F. W. Zwiers, X. Zhang, and G. C. Hegerl, 2007: Changes in Temperature and Precipitation Extremes in the IPCC Ensemble of Global Coupled Model Simulations. *Journal of Climate*, **20**, 1419–1444.

Lorenz, D. J. and E. T. DeWeaver, 2007: The Response of the Extratropical Hydrological Cycle to Global Warming. *Journal of Climate*, **20**, 3470–3484.

Lu, J., G. Chen, and D. M. W. Frierson, 2008: Response of Zonal Mean Atmospheric Circulation to El Niño versus Global Warming. *Journal of Climate*, **21**, 5835–5851.

Massey, F. J., 1951: The Kolmogorov-Smirnov Test for Goodness of Fit. *Journal of the American Statistical Association*, **46 (253)**, 68–78.

Mo, K. C. and R. W. Higgins, 1998: Tropical Influences on California Precipitation. *Journal of Climate*, **11**, 412–430.

O'Gorman, P. A. and T. Schneider, 2009: Scaling of Precipitation Extremes over a Wide Range of Climates Simulated with an Idealized GCM. *Journal of Climate*, **22**, 5676–5685.

Pall, P., M. R. Allen, and D. A. Stone, 2007: Testing the Clausius-Clapeyron constraint on changes in extreme precipitation under co_2 warming. *Climate Dynamics*, **28**, 351–363.

Sardeshmukh, P. D., G. P. Compo, and C. Penland, 2000: Changes of Probability Associated with El Niño. *Journal of Climate*, **13**, 4268–4286.

Schonher, T. and S. E. Nicholson, 1989: The Relationship between California Rainfall and ENSO events. *Journal of Climate*, **2**, 1258–1269.

Solomon, S., D. Qin, M. Manning, Z. Chen, M. Marquis, K. Averyt, M. Tignor, and H. Miller, (Eds.) , 2007: *Climate Change 2007: The Physical Science Basis. Contribution of Working Group I to the Fourth Assessment Report of the Intergovernmental Panel on Climate Change*. Cambridge University Press, Cambridge, United Kingdom and New York, NY, USA, 996 pp.

Stephens, M. A., 1979: Use of the Kolmogorov-Smirnov, Cramer-Von Mises and Related

Statistics Without Extensive Tables. *Journal of the Royal Statistical Society Series B (Methodological)*, **32**, 115–122.

Sun, Y., S. Solomon, A. Dai, and R. W. Portmann, 2006: How Often Does It Rain? *Journal of Climate*, **19**, 916–934.

Sun, Y., S. Solomon, A. Dai, and R. W. Portmann, 2007: How Often Will It Rain? *Journal of Climate*, **20**, 4801–4818.

Trenberth, K. E., 1997: The Definition of El Niño. *Bulletin of the American Meteorological Society*, **78**, 2771–2777.

Trenberth, K. E., A. Dai, R. M. Rasmussen, and D. B. Parsons, 2003: The Changing Character of Precipitation. *Bulletin of the American Meteorological Society*, **84**, 1205–1217.

van Oldenborgh, G. J., S. Y. Philip, and M. Collins, 2005: El Niño in a changing climate: a multi-model study. *Ocean Science*, **1**, 81–95.

von Storch, H. and F. W. Zwiers, 1999: *Statistical Analysis in Climate Research*. Cambridge University Press, Cambridge, United Kingdom and New York, NY, USA, 484 pp.

Wentz, F. J., L. Ricciardulli, K. Hilburn, and C. Mears, 2007: How Much More Rain Will Global Warming Bring? *Science*, **317**, 233–235.

Wilby, R. L. and T. M. L. Wigley, 2002: Future changes in the distribution of daily precipitation totals across North America. *Geophysical Research Letters*, **29 (7)**.

Wilcox, E. M. and L. J. Donner, 2007: The Frequency of Extreme Rain Events in Satellite Rain-Rate Estimates and an Atmospheric General Circulation Model. *Journal of Climate*, **20**, 53–69.

Zhou, Y. P., et al., 2007: Use of High-Resolution Satellite Observations to Evaluate Cloud and Precipitation Statistics from Cloud-Resolving Model Simulations. Part I: South China Sea Monsoon Experiment. *Journal of the Atmospheric Sciences*, **64**, 4309–4329.

List of Tables

Table 1. List of warm and cold event years (corresponding to the January months) during 1950-2008. The year is considered warm (cold) when the NDJFM average of the Niño 3.4 SST anomaly index exceeds 1K (-1K). Recall that the precipitation dataset only extends through 1998.

warm (El Niño)	cold (La Niña)
1958	1950
1966	1956
1973	1971
1983	1974
1987	1976
1992	1985
1995	1989
1998	1999
2003	2000
-	2008

Table 2. Kolmogorov-Smirnov test statistic D_{ks} indicating the maximum separation between warm and cold event distributions (Figure 6). In parentheses is the test statistic for precipitation distributions relative to mean daily precipitation intensity (Figure 7). The critical value of the test statistic required to accept the null hypothesis is 0.0506 at the 5% significance level.

	Southwest	Northwest
Fraction of rainy days	0.116 (0.076)	0.095 (0.035)
Fraction of total rain	0.099 (0.128)	0.103 (0.070)

List of Figures

4 Results of t test showing regions of statistically-significant change in mean daily precipitation intensity during ENSO events, after correcting for temporal correlation at each grid cell. Shading indicates the p-value for the left-tail test. In other words, $p = 0.95$ represents an increase in intensity during warm (relative to cold) events at the 5% significance level, and $p = 0.05$ represents an increase during cold (relative to warm) events, also at the 5% significance level. The significance level is the probability of incorrectly rejecting the null hypothesis. 47

5 Results of K-S test applied to distributions of the fraction of rainy days (*top*) and the fraction of total rain (*bottom*). The left panel shows regions of statistically-significant shifts in the warm ENSO event distribution towards more intense daily rainfall rates, relative to the cold event distribution. The right panel shows the same for cold relative to warm events. Shading indicates the 5% significance level. At some grid cells, primarily in the SW, the K-S test returns a significant result in both cases (compare c and d). This can only occur when the cumulative distributions intersect in the middle of the distribution, meaning that warm event precipitation significantly exceeds cold event precipitation at one point ($f(x_1) > g(x_1)$ in Equation 1), and vice versa at another ($f(x_2) < g(x_2)$). 48

6 Distributions of regional-mean precipitation for warm (solid) and cold (dashed) ENSO events, including mean daily precipitation intensity (vertical lines) and 95% confidence limits (gray envelope) for the K-S test. A shift in the distribution towards more intense daily rainfall rates implies an increase in the fraction of rainy days or total rain contributed by heavy precipitation. Test statistics are given in Table 2. 49

7 Normalized distributions of regionally-averaged precipitation for warm (solid) and cold (dashed) ENSO events, and 95% confidence limits (gray envelope) for the K-S test. Test statistics are given in Table 2. We normalize the x axis for each distribution such that a value of one equals the mean daily rainfall rate (and a value of two is twice the mean daily rainfall rate). 50

8 Mean daily aggregate rainfall rate for warm minus cold ENSO events as a function of threshold for the NW (a) and SW (b). This aggregate reflects an integrative measure of precipitation rates in the tail of the distributions beyond the specified threshold. We run t tests on categories of daily rainfall rates, testing every precipitation threshold in increments of 1 mm/day. The gray envelope indicates 95% confidence limits for the two-sample t test, after correcting for spatial and temporal correlation. The dashed envelope represents our most conservative estimate, assuming perfect spatial correlation. For thresholds greater than $\sim$20 mm/day, cold events show a significant increase in mean daily intensity relative to warm events in the SW regional average. 51

9 Wintertime precipitation differences for warm minus cold ENSO events. (a) Percent difference in mean daily precipitation intensity. (b) Percent difference in number of rainy days. All precipitation events less than 20 mm/day per grid cell have been excluded. In general, as the precipitation threshold is raised there are increasingly larger regions for which no heavy precipitation is observed during ENSO. Thus we note that for precipitation $\geq$20 mm/day, the difference in mean daily intensity cannot be calculated for portions of the western U.S. interior. 52

A1 (a) Aggregate number of rainy days as a function of threshold for warm (solid) and cold (dashed) ENSO events. (b) Same but for the fraction of rainy days. 53

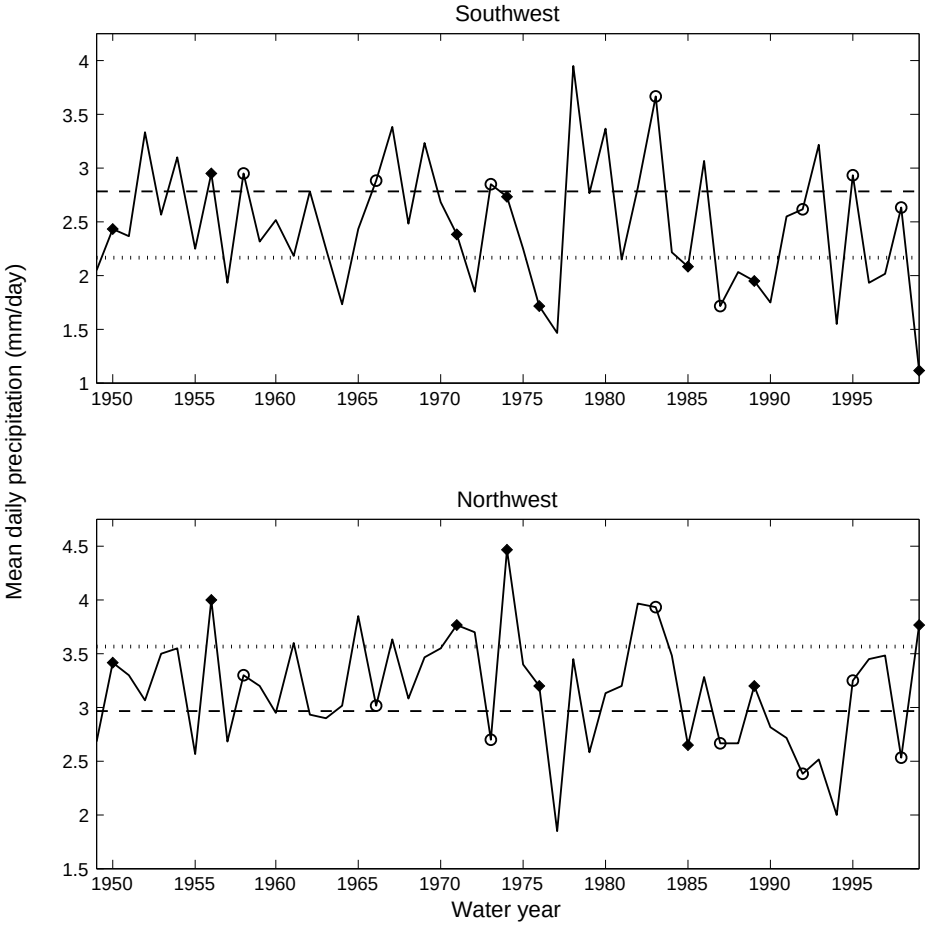

Fig. 1. Wintertime-mean daily precipitation time series averaged over the southwest (SW) and northwest (NW) regions. Filled diamonds indicate strong La Niña events, open circles indicate strong El Niño events. Dashed (dotted) lines represent the mean wintertime precipitation for all El Niño (La Niña) winters averaged over each region.

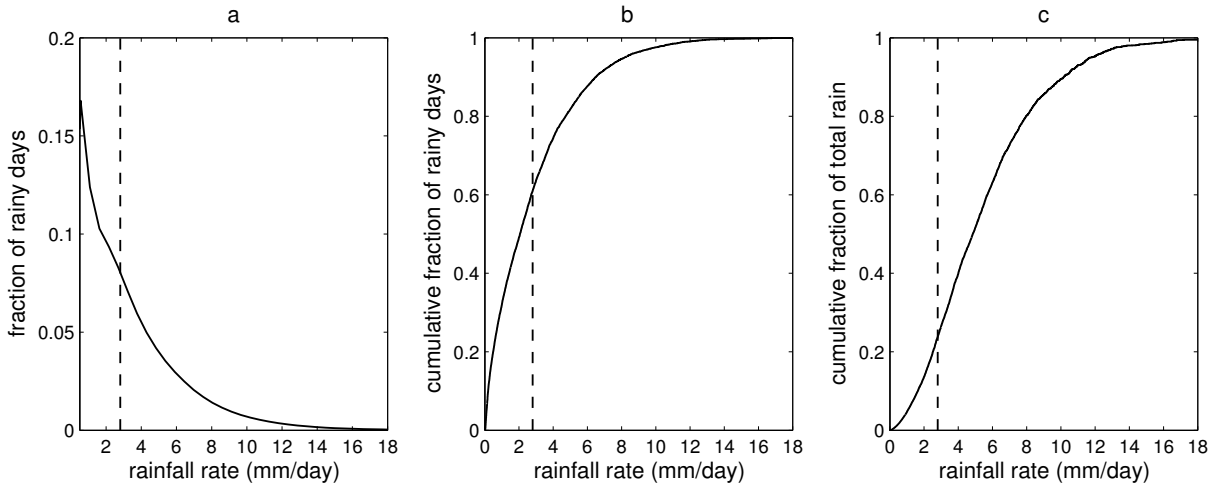

Fig. 2. Climatological wintertime-mean daily precipitation in the NW during NDJFM (40-49.5°N, 110-126.25°W), presented as a (a) density distribution of regionally-averaged precipitation, (b) cumulative distribution of fraction of rainy days, and (c) cumulative distribution of fraction of total rain amount, all as a function of rainfall rate.

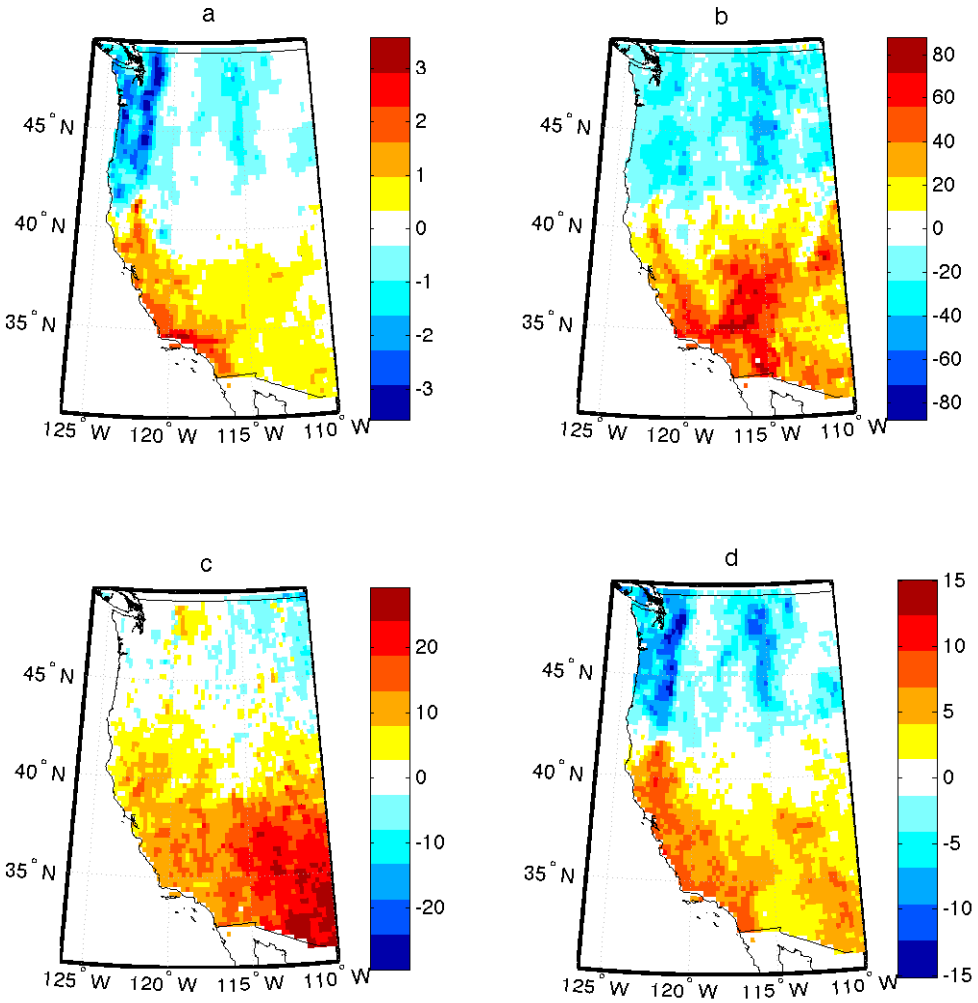

Fig. 3. Wintertime (NDJFM) precipitation differences for warm minus cold ENSO events. (a) Difference in mean daily precipitation when raining, in mm. (b) Percent difference in mean daily precipitation when raining. (c) Percent difference in number of rainy days. (d) Percent difference in number of rainy days with precipitation $\geq$5 mm/day.

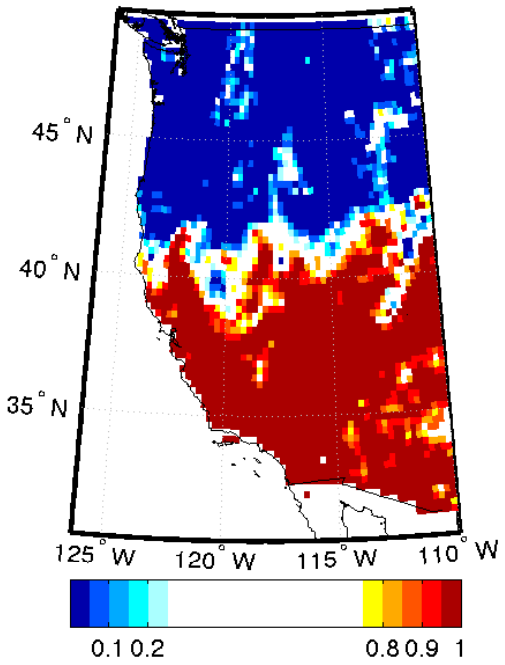

Fig. 4. Results of t test showing regions of statistically-significant change in mean daily precipitation intensity during ENSO events, after correcting for temporal correlation at each grid cell. Shading indicates the p-value for the left-tail test. In other words, $p = 0.95$ represents an increase in intensity during warm (relative to cold) events at the 5% significance level, and $p = 0.05$ represents an increase during cold (relative to warm) events, also at the 5% significance level. The significance level is the probability of incorrectly rejecting the null hypothesis.

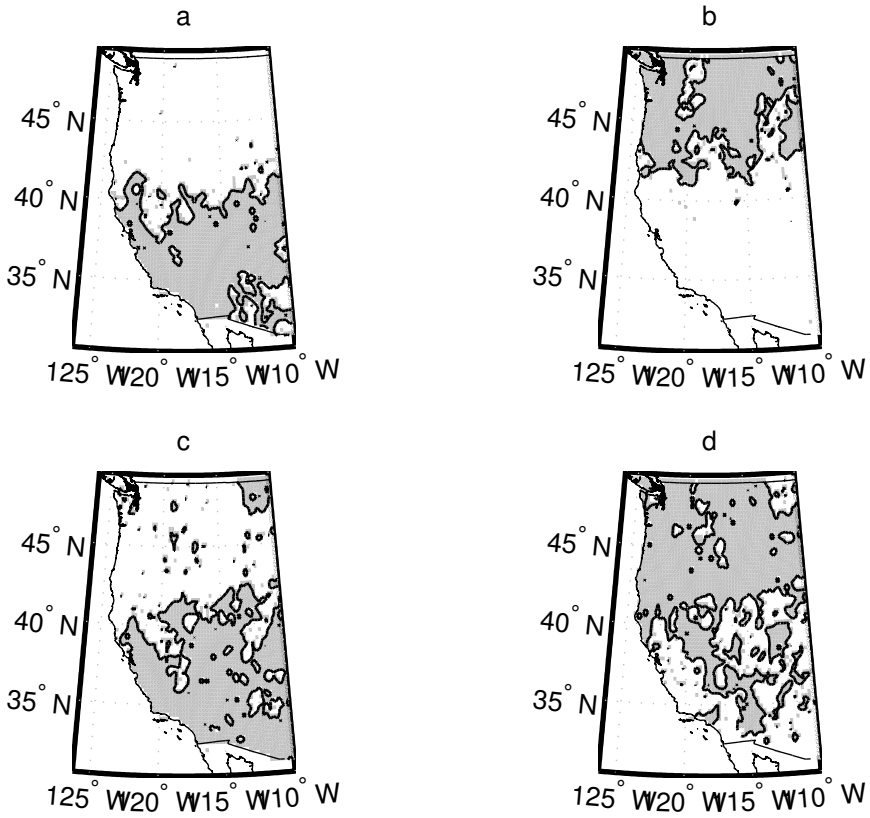

Fig. 5. Results of K-S test applied to distributions of the fraction of rainy days (*top*) and the fraction of total rain (*bottom*). The left panel shows regions of statistically-significant shifts in the warm ENSO event distribution towards more intense daily rainfall rates, relative to the cold event distribution. The right panel shows the same for cold relative to warm events. Shading indicates the 5% significance level. At some grid cells, primarily in the SW, the K-S test returns a significant result in both cases (compare c and d). This can only occur when the cumulative distributions intersect in the middle of the distribution, meaning that warm event precipitation significantly exceeds cold event precipitation at one point ($f(x_1) > g(x_1)$ in Equation 1), and vice versa at another ($f(x_2) < g(x_2)$).

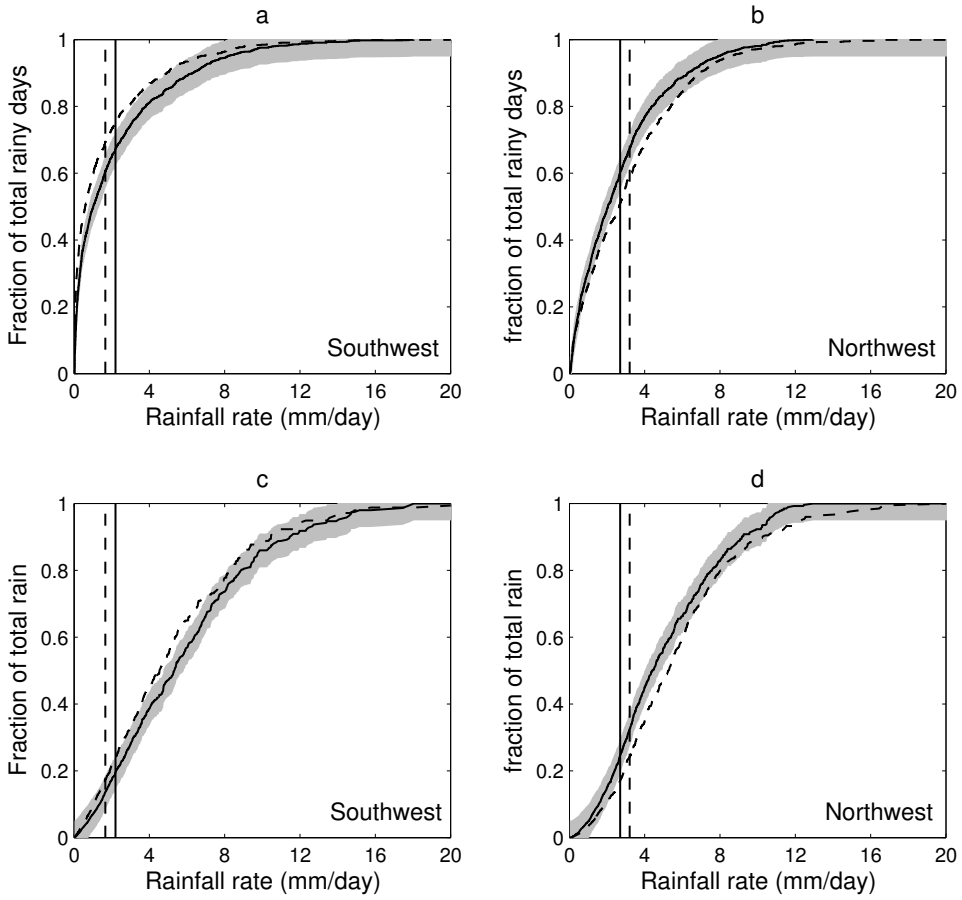

Fig. 6. Distributions of regional-mean precipitation for warm (solid) and cold (dashed) ENSO events, including mean daily precipitation intensity (vertical lines) and 95% confidence limits (gray envelope) for the K-S test. A shift in the distribution towards more intense daily rainfall rates implies an increase in the fraction of rainy days or total rain contributed by heavy precipitation. Test statistics are given in Table 2.

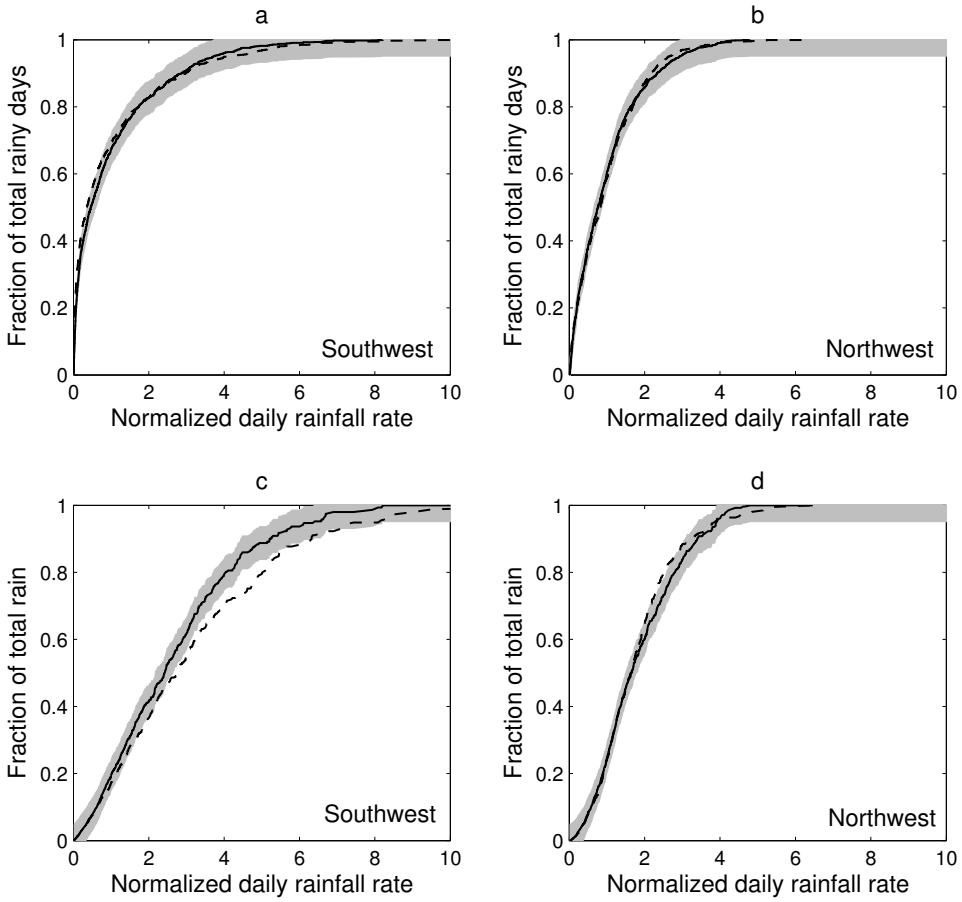

Fig. 7. Normalized distributions of regionally-averaged precipitation for warm (solid) and cold (dashed) ENSO events, and 95% confidence limits (gray envelope) for the K-S test. Test statistics are given in Table 2. We normalize the x axis for each distribution such that a value of one equals the mean daily rainfall rate (and a value of two is twice the mean daily rainfall rate).

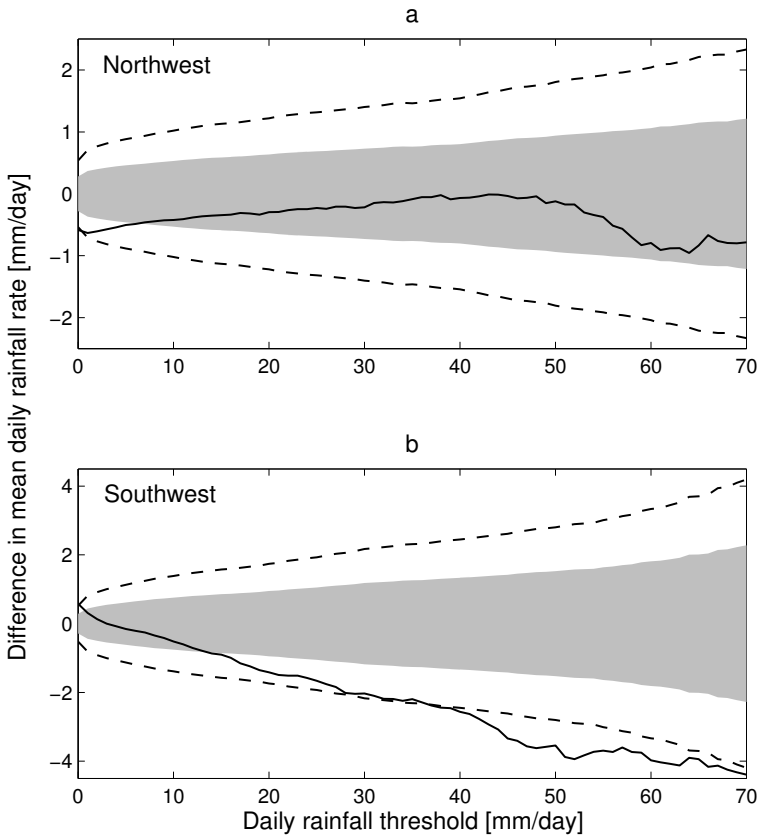

Fig. 8. Mean daily aggregate rainfall rate for warm minus cold ENSO events as a function of threshold for the NW (a) and SW (b). This aggregate reflects an integrative measure of precipitation rates in the tail of the distributions beyond the specified threshold. We run t tests on categories of daily rainfall rates, testing every precipitation threshold in increments of 1 mm/day. The gray envelope indicates 95% confidence limits for the two-sample t test, after correcting for spatial and temporal correlation. The dashed envelope represents our most conservative estimate, assuming perfect spatial correlation. For thresholds greater than $\sim$20 mm/day, cold events show a significant increase in mean daily intensity relative to warm events in the SW regional average.

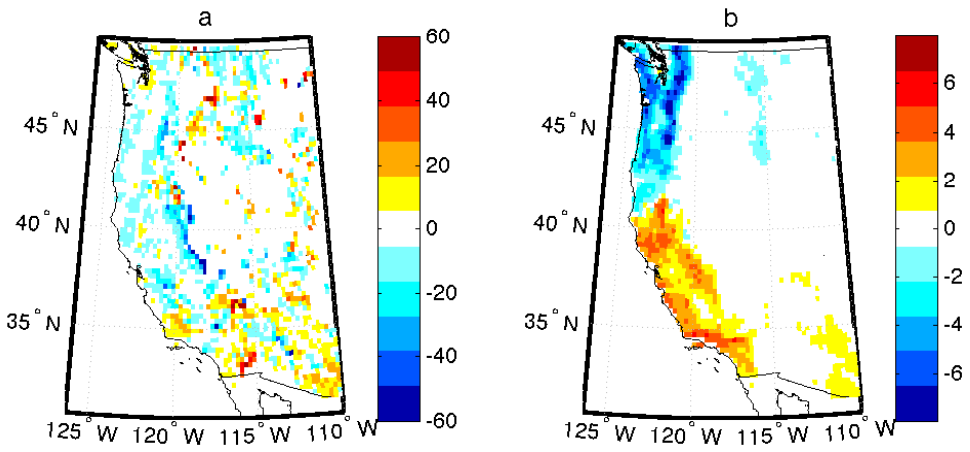

Fig. 9. Wintertime precipitation differences for warm minus cold ENSO events. (a) Percent difference in mean daily precipitation intensity. (b) Percent difference in number of rainy days. All precipitation events less than 20 mm/day per grid cell have been excluded. In general, as the precipitation threshold is raised there are increasingly larger regions for which no heavy precipitation is observed during ENSO. Thus we note that for precipitation $\geq$20 mm/day, the difference in mean daily intensity cannot be calculated for portions of the western U.S. interior.

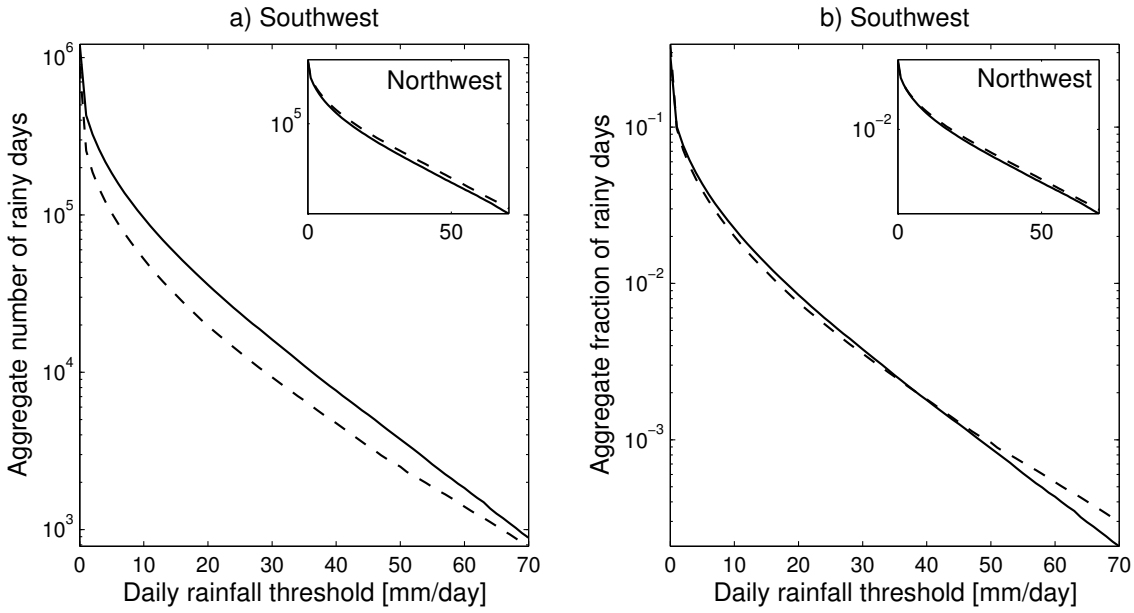

Fig. A1. (*a*) Aggregate number of rainy days as a function of threshold for warm (solid) and cold (dashed) ENSO events. (*b*) Same but for the fraction of rainy days.